# Vacuum ultraviolet and visible spectra of ZnO:Eu$^{3+}$ prepared by combustion synthesis

# Vacuum ultraviolet and visible spectra of ZnO:Eu$^{3+}$ prepared by combustion synthesis

**Bing-Ming Cheng**[1]**, Lixin Yu**[2]**, Chang-kui Duan**[2]**, Huaishan Wang**[2]
**and Peter A Tanner**[2,3]

[1] National Synchrotron Radiation Research Centre, Hsinchu, Taiwan
[2] Department of Biology and Chemistry, City University of Hong Kong, Kowloon, Hong Kong

E-mail: bhtan@cityu.edu.hk

**Abstract**
Zinc oxide doped with 1 at.% Eu$^{3+}$ has been prepared by combustion synthesis using several
different reductants. Samples sintered at 800 °C were ∼30 nm in size and Fourier transform IR
spectra demonstrated that they were relatively free of contaminants. Ultraviolet and
near-ultraviolet laser excited emission spectra showed that Eu$^{3+}$ ions are disordered and not
situated at discrete lattice sites in ZnO and consequently no evidence for energy transfer from
the host to Eu$^{3+}$ was found. Vacuum ultraviolet (VUV) excitation produced defect site emission
in addition to near-band-edge emission but the intensity of the Eu$^{3+}$ visible emission was very
weak. Bands between 6.2 and 9.1 eV in the VUV excitation spectra have been assigned to
electric dipole allowed transitions, 3d–4p.

(Some figures in this article are in colour only in the electronic version)

## 1. Introduction

The bandgap of ZnO is at ∼3.37 eV (∼27 181 cm$^{-1}$; 368 nm)
and some studies have explored the possibility of incorporating
lanthanide ions (Ln$^{3+}$) into this host and obtaining sharp
luminescence spectra via excitation into the ZnO host with
subsequent energy transfer [1–13]. The synthesis techniques
for doped zinc oxide have employed spray pyrolysis [9],
hydrothermal synthesis [13] or a microemulsion method [10]
for control of morphology, sol–gel methods [5, 6], powder
sintering [7, 8, 11], implantation [3], or vapour deposition [1].
The ionic radius of Zn$^{2+}$ is 72 pm, and therefore besides charge
compensation there are also steric problems in doping Ln$^{3+}$,
such as Er$^{3+}$ (89 pm) or Eu$^{3+}$ (95 pm), into the crystal lattice.
Zinc ions are tetrahedrally coordinated so Ln$^{3+}$ must reside
at an alternative site to satisfy coordination saturation from
sixfold to ninefold. Consequently there have been conflicting
reports as to whether or not the Ln$^{3+}$ is located at a specific
site within the ZnO lattice or if it is present in a disordered
structure. Some authors have reported efficient energy transfer

from the ZnO host to Ln$^{3+}$ which results in bright 4f$^N$–4f$^N$
emission [5, 8] whereas others asserted the absence of efficient
energy transfer [6]. Generally, it was found that weak Eu$^{3+}$
emission is superimposed upon broadband defect emission and
the wavelengths of the Eu$^{3+}$ luminescence bands depend upon
the nature of the starting material.

Combustion synthesis of ZnO generally gives clusters
of particles or thin flakes [14], although nearly hexagonal
nanocrystalline particles have been obtained with careful
control of the reactant composition [15]. To our knowledge,
the optical properties of ZnO:Ln$^{3+}$ prepared by combustion
synthesis have not previously been investigated; this is the
subject of the present study, which focuses upon Ln = Eu.

## 2. Experimental details

Zinc nitrate hexahydrate, glycine, urea and hydrazine hydrate
(all analytical reagents) and Eu$_2$O$_3$ (Strem, 99.99%) were used
as starting materials for the syntheses of doped zinc oxide
nanocrystals. In a typical synthesis, 0.0181 g Eu$_2$O$_3$ was
dissolved in dilute HNO$_3$ first and then Zn(NO$_3$)$_2$·6H$_2$O and

---

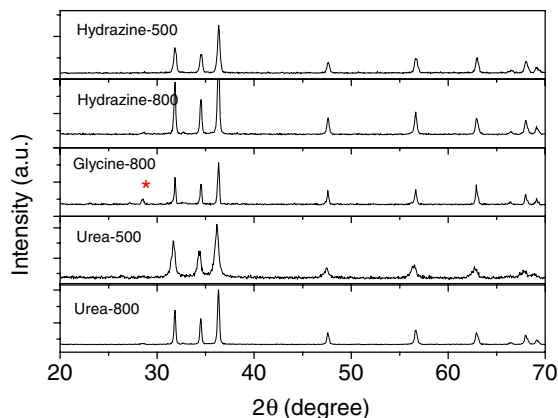[3] Author to whom any correspondence should be addressed.

**Figure 1.** The x-ray diffraction patterns of ZnO:Eu$^{3+}$ (1 at.%) prepared by combustion synthesis with different fuels, and sintering temperatures in °C, as indicated.



**Figure 2.** FTIR spectra of KBr discs of ZnO and ZnO:Eu$^{3+}$ nanostructures. Top spectra, neat ZnO; bottom spectra, ZnO doped with 1 at.% Eu$^{3+}$, prepared using the following reductants and temperatures: (a) urea, 800 °C; (b) glycine, 800 °C; (c) hydrazine, 500 °C; (d) hydrazine, 800 °C. The absorption at ~2330 cm$^{-1}$ is an artefact due to atmospheric CO$_2$.
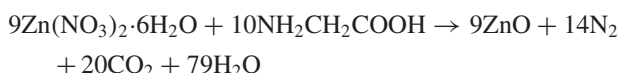
fuel (glycine, urea or hydrazine hydrate) were added to the above solution and were heated (the mole ratio of Eu to Zn was 0.01). The powders were calcined at 500 or 800 °C for 1 h to remove nitrate and organic substances. The powders obtained were then sealed until measurement. Neat ZnO nanocrystals were prepared with the same procedure, in the absence of Eu$_2$O$_3$.

The structure of these samples was determined by means of powder XRD with a Siemens D500 x-ray diffractometer. FTIR spectra of samples in KBr discs were recorded using Nicolet 360 and Perkin-Elmer 1600 spectrometers at room temperature. The visible emission spectra were recorded at resolution 4 cm$^{-1}$ using an Acton 0.5 m monochromator and a back-illuminated SpectruM CCD detector, using the third harmonic of a Surelite Nd:YAG pulsed laser (355 nm) or an argon ion laser (465 nm).

Emission and excitation spectra were recorded at a resolution of 0.3–2.5 nm at room temperature using the photoluminescence end station coupled to the high flux BL03A synchrotron radiation beam line at the National Synchrotron Radiation Research Centre, Hsinchu, Taiwan.

## 3. Results and discussion

In the combustion process, Zn(NO$_3$)$_2$ was the zinc source and oxidant, and the fuel was the reductant. The typical combustion reactions with different reductants are listed as follows:

$$9Zn(NO_3)_2 \cdot 6H_2O + 10NH_2CH_2COOH \rightarrow 9ZnO + 14N_2$$
$$+ 20CO_2 + 79H_2O$$
$$3Zn(NO_3)_2 \cdot 6H_2O + 5CO(NH_2)_2 \rightarrow 3ZnO + 5CO_2$$
$$+ 8N_2 + 18H_2O$$
$$2Zn(NO_3)_2 \cdot 6H_2O + 5N_2H_2 \cdot H_2O \rightarrow 9ZnO + 7N_2 + 22H_2O.$$

The equivalent stoichiometric ratio of fuel to Zn(NO$_3$)$_2$·6H$_2$O which was employed in our syntheses was 1.11, 1.67 and 2.5 for glycine, urea and hydrazine hydrate, respectively. To determine the size and structures of samples, their x-ray powder diffraction was investigated and the undoped ZnO samples showed the wurtzite structure (JCPDF 79-206)
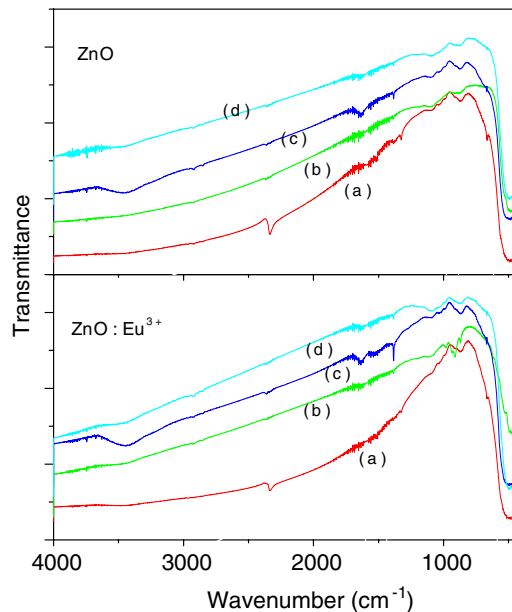
without any additional lines (not shown). According to figure 1, the structures of all doped samples at 1 at.% Eu$^{3+}$ (labelled ZnO:Eu$^{3+}$ in the following) also belonged to the hexagonal phase and no characteristic diffraction peaks of Eu$_2$O$_3$ were observed. However, the absence of such peaks at the dopant level of 1 at.% may be expected from the sensitivity of these x-ray powder diffractograms. The particle size was determined by using the strongest diffraction peak at 36.3° (101) with the Scherrer equation and was determined as 17 nm for ZnO:Eu$^{3+}$ sintered at 500 °C with urea as fuel, and about 31 nm for the other samples sintered at 800 °C. An additional unknown peak was observed for the sample synthesized with glycine as fuel (labelled with a star).

A more sensitive test of the purity of the samples is achieved from their FTIR spectra, shown for the ZnO and ZnO:Eu$^{3+}$ nanostructures sintered at 800 °C in figure 2. The zinc oxide fundamental vibrational absorptions are at <520 cm$^{-1}$, whereas other absorption bands refer to the presence of the following trace impurities: 3450–3500 cm$^{-1}$ and 1630 cm$^{-1}$, water; 1385 cm$^{-1}$, adsorbed nitrate ions in figures 2(b) and (c); and there is a weak peak at 1323 cm$^{-1}$ in figure 2(a) which is not unambiguously assigned. The samples sintered at 500 °C show intense absorption bands due to the presence of residual organic matter. In view of these impurities these samples were not considered further.

The room temperature 355 nm excited photoluminescence spectra of ZnO:Eu$^{3+}$ for the samples prepared using glycine and urea sintered at 800 °C are similar and the spectrum of the former sample is shown in figure 3(a). One band with maximum at 387 ± 2 nm and FWHM 15 nm is observed in each case, corresponding to near-band-edge emission of ZnO.
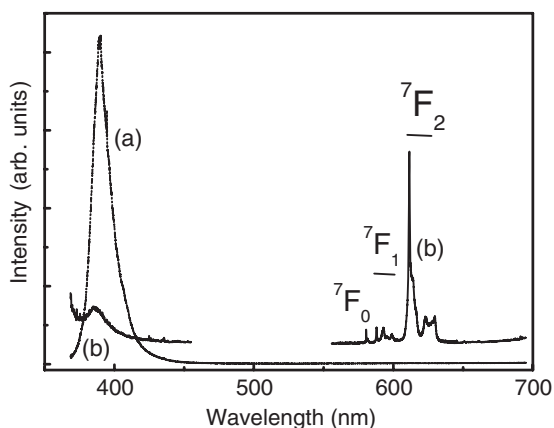
**Figure 3.** Room temperature 355 nm excited emission spectra between 380 and 700 nm of (a) ZnO:Eu$^{3+}$ (1 at.%) prepared using the reductant glycine, with the sintering temperature at 800 °C; (b) C-type Eu$_2$O$_3$ (Aldrich, 99.999%). The initial luminescent state in (b) is $^5D_0$ and the terminal multiplet states are marked in the figure.



**Figure 4.** 464.5 nm excited emission spectra between 560 and 645 nm of C-type Eu$_2$O$_3$; a ground mixture of (1 at.% Eu:Zn) C-type Eu$_2$O$_3$ and ZnO after heating to 800 °C for 1 h; samples of ZnO:Eu$^{3+}$ (1 at.%) prepared by the glycine and urea combustion syntheses and sintered at 800 °C for 1 h.

Although no emission from Eu$^{3+}$ is evident in figure 3(a), some samples exhibited very weak emission from $^5D_0$ under these conditions. However, even the presence of very weak emission from Eu$^{3+}$ does not support the conclusion of energy transfer from the host to the Eu$^{3+}$ activator ion. The 355 nm excited emission spectrum of C-type Eu$_2$O$_3$ alone (without further treatment: Aldrich, 99.999%) was recorded (figure 3(b)) and exhibits luminescence under this excitation wavelength. The most intense luminescence originates from the $^5D_0$ electronic state and the band assignments for the terminal multiplet states [16] are marked in the figure. Figure 4 shows the room temperature emission spectra of the glycine (a) and urea (b) ZnO:Eu$^{3+}$ samples calcined at 800 °C under excitation directly into $^5D_2$ using 464.5 nm radiation. Also shown, for comparison, are the corresponding spectra for C-type Eu$_2$O$_3$ powder (d), and for ZnO ground in a pestle and mortar at room temperature with (1 at.% Eu:Zn) C-type Eu$_2$O$_3$ and then heated at 800 °C for 1 h (c). The stronger, sharp bands peaking at 610 nm correspond to the $^5D_0 \rightarrow {}^7F_2$ transition [16]. A gradual blurring of features occurs on passing from the bottom spectrum to the top one. The inhomogeneous broadening is attributed to the random, disordered environment of Eu$^{3+}$ and is similar to that found in the spectra of glasses. Clearly, the Eu$^{3+}$ ion does not occupy a distinct crystallographic site in the ZnO lattice in the nanocrystals. Thus, there is a phase separation in the nanomaterials and the Eu$^{3+}$ ions are not situated at well-defined sites within the ZnO lattice. The preparations using glycine or urea were repeated and the resulting spectra were similar but not identical to those in figure 4, since they showed different extents of inhomogeneous broadening.

The synchrotron radiation excited emission and excitation spectra of the samples prepared using glycine and urea and sintered at 800 °C were also recorded at room temperature and are shown in figures 5 and 6, respectively. The emission bands are mainly from defect lattice sites of ZnO, except for the near-band-edge emission at ∼381 nm, and have been a common feature in the photoluminescence studies of ZnO (e.g. [17, 18])
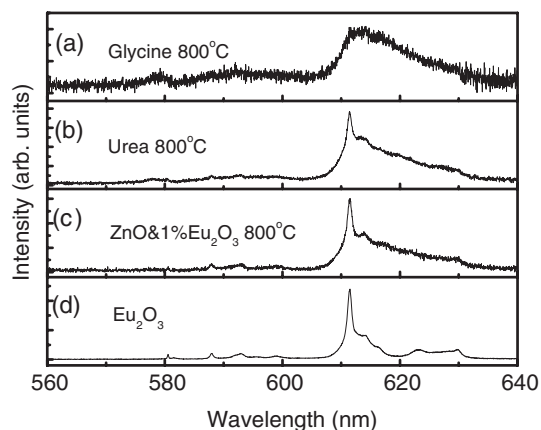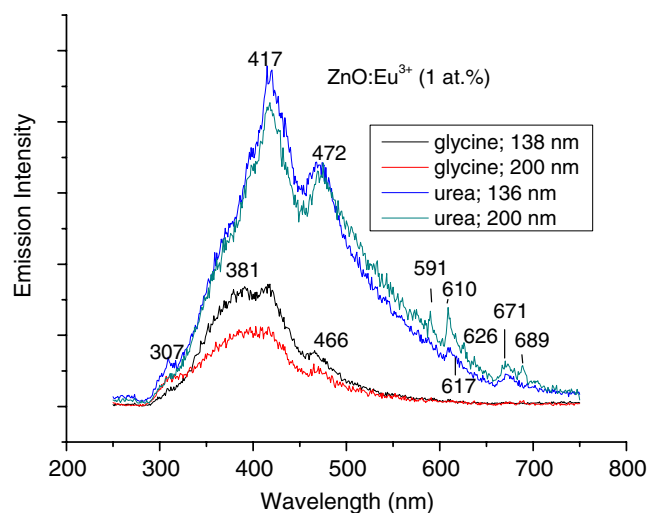


**Figure 5.** Emission spectra of ZnO:Eu$^{3+}$ (1 at.%) samples prepared using glycine or urea and sintered at 800 °C, excited by 136, 138 or 200 nm synchrotron radiation. Band maxima are given in nanometres.

with various explanations. We do not attempt to make specific assignments but note that the relative intensities of the bands at 381, 417 and ∼470 nm are different in the samples prepared using glycine and urea. By contrast, the intensities of the Eu$^{3+}$ emission bands from the $^5D_0$ initial state are very weak. The energy transfer from host or defect states to Eu$^{3+}$ is therefore not efficient, as deduced above. The excitation spectra of emission from these two samples, figure 6, exhibit different features at 307 nm (urea) and 333 nm (glycine), which correspond to defect site absorptions. However, bands with similar intensity ratios in each spectrum are observed at 200 nm (6.20 eV), 170 nm (7.3 eV) and 136 nm (9.1 eV) which are associated with electronic transitions of ZnO. Calculation [19] showed that the conduction band (CB) is composed of 2p orbitals of O and 4s–4p hybrid orbitals of Zn, and the valence band (VB) is composed of 2p orbitals of O and 3d orbitals of Zn. Under the tight binding approximation, the transition
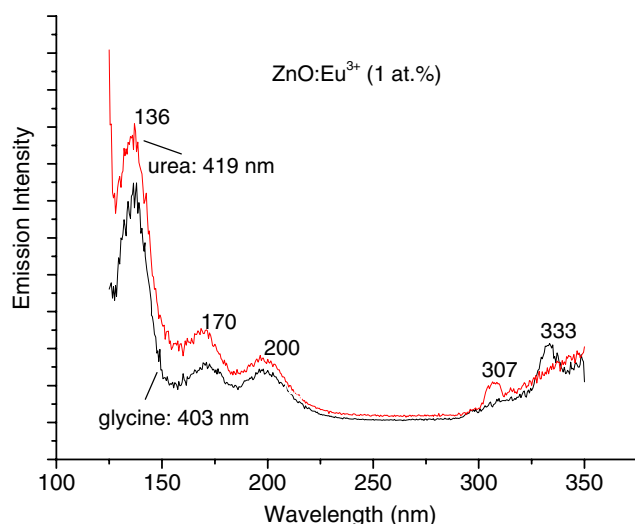
**Figure 6.** Excitation spectra of ZnO:$Eu^{3+}$ samples prepared using glycine or urea and sintered at 800 °C, monitoring 403 nm and 419 nm emission, respectively. Band maxima are given in nanometres.

between the VB and CB is mainly due to the electric dipole moment, between 3d and 4p orbitals of Zn. The calculated 3d partial density of states (PDOS) gave three peaks at −4, −2.2 and −1.2 eV relative the top of the VB. Hence, the three peaks at 136, 170 and 200 nm are interpreted as VB to CB transitions due to the electric dipole moment between 3d and 4p orbitals in ZnO. The excitation spectrum here is compared to VUV absorption or excitation spectra reported previously for various samples: VUV absorption for films deduced from reflection spectra [20] showed 6.1–7.5 eV and ∼10 eV peaks; excitation spectra detecting UV emission for film [21] and powder [22] samples showed broad peaks at 197 nm (6.3 eV) and 161 nm (7.7 eV), respectively.

## 4. Conclusions

We previously found that $\alpha$-$Al_2O_3$ did not incorporate $Ln^{3+}$ into the crystal lattice when prepared by soft sol–gel synthesis [23], but that the use of combustion synthesis enabled $Eu^{3+}$ to occupy a $C_{3v}$ symmetry site [24]. This prompted the use of combustion synthesis in the case of ZnO:$Eu^{3+}$. However it is clear from the luminescence spectra that $Eu^{3+}$ retains the coordination of C-type $Eu_2O_3$ but is distorted to varying extents by nearest-neighbour environments. These results provide a similar conclusion to those using hydrothermal synthesis for ZnO:$Eu^{3+}$ [13]. Recently, Liu *et al* have employed a modified sol–gel procedure to prepare ∼9 nm nanocrystals of ZnO:$Eu^{3+}$ [12, 25] and in addition to the occupation of distorted lattice sites by $Eu^{3+}$, it was proposed that $Eu^{3+}$ enters a well-defined lattice site when the sintering temperature <500 °C. Clearly the addition of $Li^+$ in their synthesis results in the rather different luminescence spectra and in the integrity of the 'ZnO:$Eu^{3+}$'. In the present study, various laser excitation lines from VUV to the near-ultraviolet

have been employed and the $^5D_0$ emission spectra of $Eu^{3+}$ comprise weak and broad features. Defect site red or green emission was not evident from ZnO:$Eu^{3+}$ under 355 nm or 464.5 nm excitation, but blue defect site emission was apparent under VUV excitation. Features in the VUV excitation spectra between 136 and 200 nm have been assigned to electric dipole transitions of the host lattice.

## Acknowledgments

## References

[1] Armelao L, Heigl F, Jürgensen A, Blyth R I R, Regier T, Zhou X-T and Sham T K 2007 *J. Phys. Chem.* C **111** 10194
[2] Zhou Z, Komori T, Ayukawa T, Koizumi A, Matsunami N, Takeda Y and Morinaga M 2006 *Opt. Mater.* **28** 727
[3] Jadwisienczak W M, Lozykowski H J, Xu A and Patel B 2002 *J. Electron. Mater.* **31** 776
[4] Kossanyi J, Kouyate D, Pouliquon J, Ronfard-Haret J C, Oelkrug D, Mammel U, Kelly G P and Wilkinson F 1990 *J. Lumin.* **46** 17
[5] Che P, Meng J and Guo L 2007 *J. Lumin.* **122/123** 168
[6] Lima S A M, Sigoli F A, Davolos M R and Jafelicci M 2002 *J. Alloys Compounds* **344** 280
[7] Hayashi Y, Narahara H, Uchida T, Noguchi T and Ibuki S 1995 *Japan. J. Appl. Phys.* **34** 1878
[8] Park Y-K, Han J-I, Kwak M-G, Yang H, Ju S-H and Cho W-S 1998 *J. Lumin.* **78** 87
[9] Panatarani C, Lenggoro I W and Okuyama K 2004 *J. Phys. Chem. Solids* **65** 1843
[10] Ishizumi A and Kanemitsu Y 2005 *Appl. Phys. Lett.* **86** 253106
[11] Park Y-K, Han J-I, Kwak M-G, Yang H, Ju S-H and Cho W-S 1998 *Appl. Phys. Lett.* **72** 668
[12] Liu Y, Luo W, Li R, Liu G, Antonio M R and Chen X 2008 *J. Phys. Chem.* C **112** 686
[13] Tanner P A and Yu L 2008 *J. Nanosci. Nanotechnol.* **8** 1307
[14] Hwang C-C and Wu T-Y 2004 *Mater. Sci. Eng.* B **111** 197
[15] Hwang C-C and Wu T-Y 2004 *J. Mater. Sci.* **39** 6111
[16] Chen G, Haire R G and Peterson J R 1992 *Appl. Spectrosc.* **46** 273
[17] Leung Y H, Djurisic A B, Liu Z T, Li D, Xie M H and Chan W K 2008 *J. Phys. Chem. Solids* **69** 353
[18] Ghosh R, Mallik B, Fujihara S and Basak D 2005 *Chem. Phys. Lett.* **403** 415
[19] Viswanatha R, Sapra S, Satpati B, Satyam P V, Dev B N and Sarma D D 2004 *J. Mater. Chem.* **14** 661
[20] Shi C, Fu Z, Guo C, Ye X, Wei Y, Deng J, Shi J and Zhang G 1999 *J. Electron Spectrosc. Relat. Phenom.* **101–103** 629
[21] Zhang G, Shi C, Han Z, Shi J, Lin B, Kirm M and Zimmerer G 2001 *Chin. J. Lumin.* **22** 157
[22] Lu C-H, Hwang W-J and Godbole S V 2005 *J. Mater. Res.* **20** 464
[23] Tanner P A, Wong K L and Liang Y 2004 *Chem. Phys. Lett.* **399** 15
[24] Tanner P A, Pan Z, Rakov N and Maciel G S 2006 *J. Alloys Compounds* **424** 347
[25] Liu Y, Luo W, Li R and Chen X 2007 *Opt. Lett.* **32** 566